Supp. Figure S1

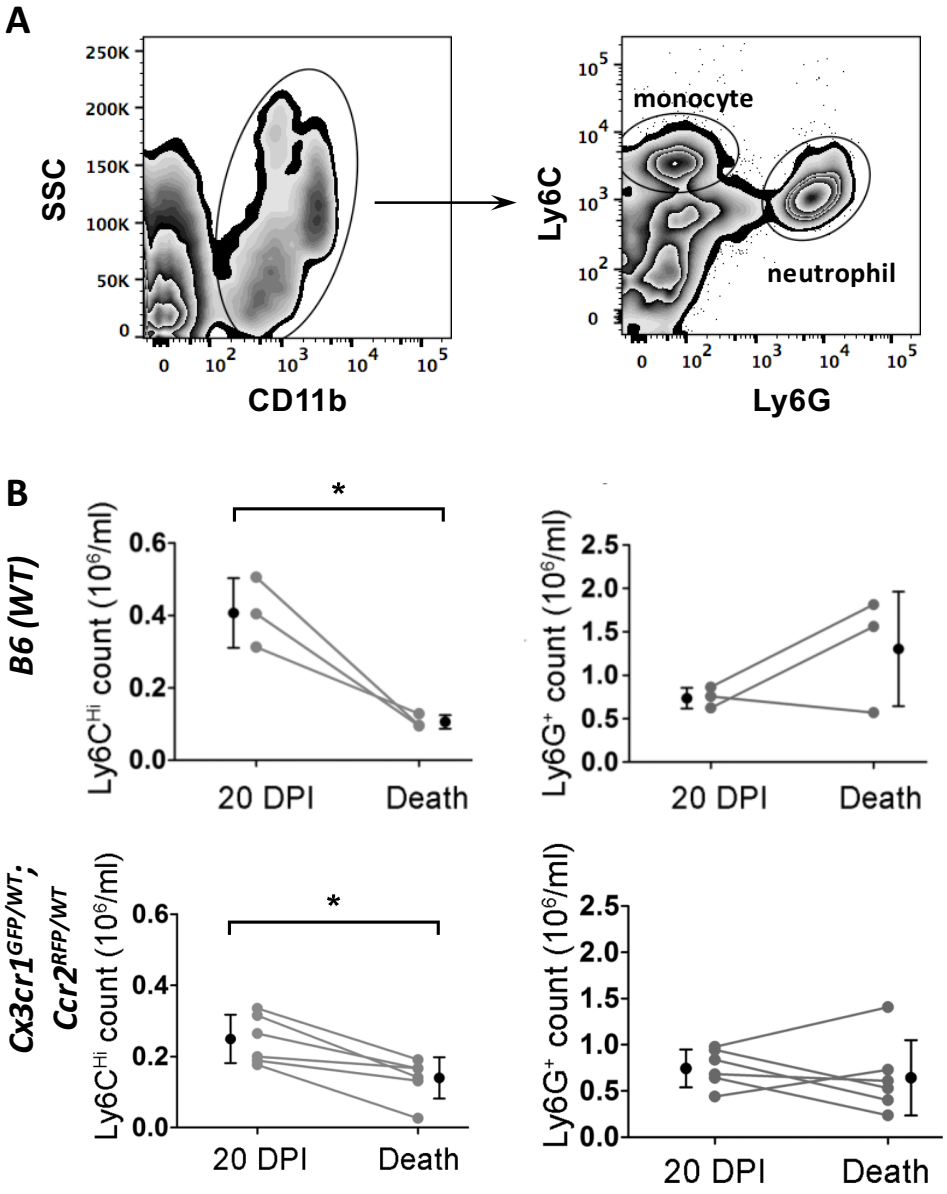

Figure S1. Circulating Ly6C^{Hi} inflammatory monocytes diminish at terminal illness. (**A**) Illustration of the FACS analysis using CD11b in combination with Ly6C and Ly6G to discriminate monocytes and neutrophils obtained from the blood. Inflammatory monocytes are CD11b^{+}Ly6C^{Hi}Ly6G^{-} cells, while neutrophils are CD11b^{+}Ly6C^{+}Ly6G^{+} cells. (**B**) Enumeration of inflammatory monocytes and neutrophils in the blood of the same mice at 20 days after (DPI) tumor cell transplantation (asymptomatic) and at the end of the survival (terminal stage of tumor development when mice were euthanized). Paired *t*-test. * $P< 0.05$. N=3 for B6 mice and 6 for *Cx3cr1*$^{GFP/WT}$;*Ccr2*$^{RFP/WT}$ mice.

Supp. Figure S2

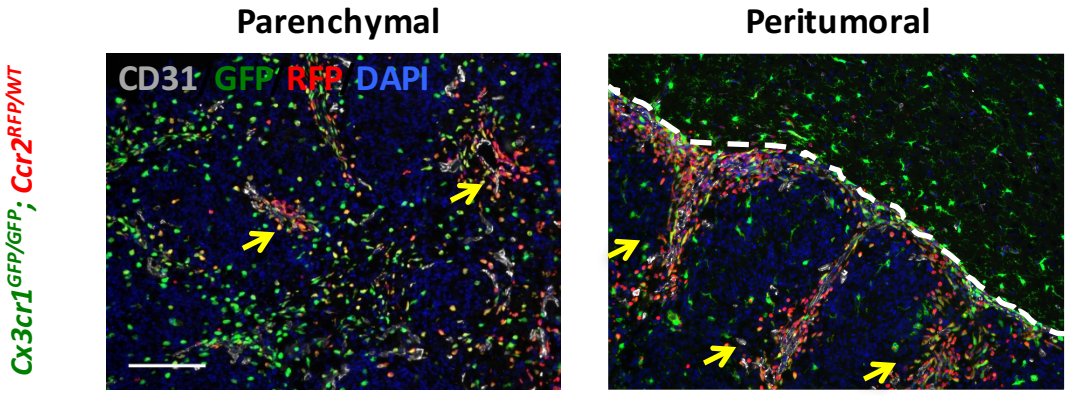

Figure S2. Enhanced BM-derived cell infiltration in *Cx3cr1*$^{GFP/GFP}$;*Ccr2*$^{RFP/WT}$ mice. GFP^{+}RFP^{+} double positive cells were found in perivascular niche in both parenchymal and peritumoral regions (arrows). Comparing to *Cx3cr1*$^{GFP/WT}$;*Ccr2*$^{RFP/WT}$ tumor, single GFP signal appeared to be increased in parenchymal region, likely due to increased GFP expression (two copies of GFP gene as compared to one). Tumor margin is marked with dotted lines.

Supp. Figure S3

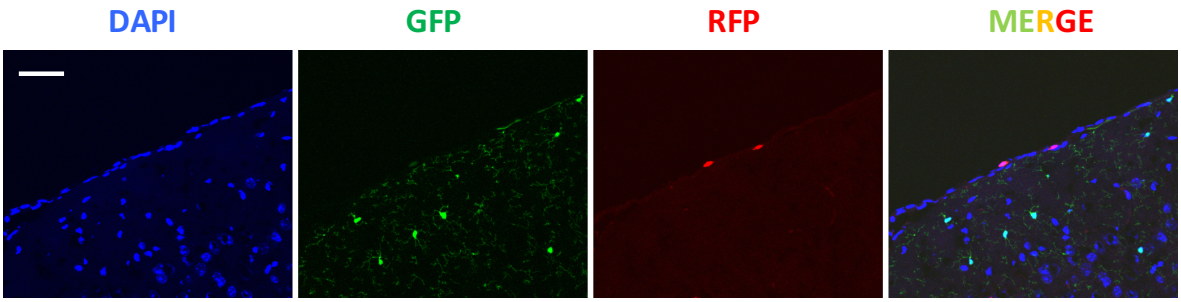

Figure S3. RFP^{+} cells are only observed in the meninges in healthy naïve *Cx3cr1*$^{GFP/WT}$;*Ccr2*$^{RFP/WT}$ mice.

Supp. Figure S4

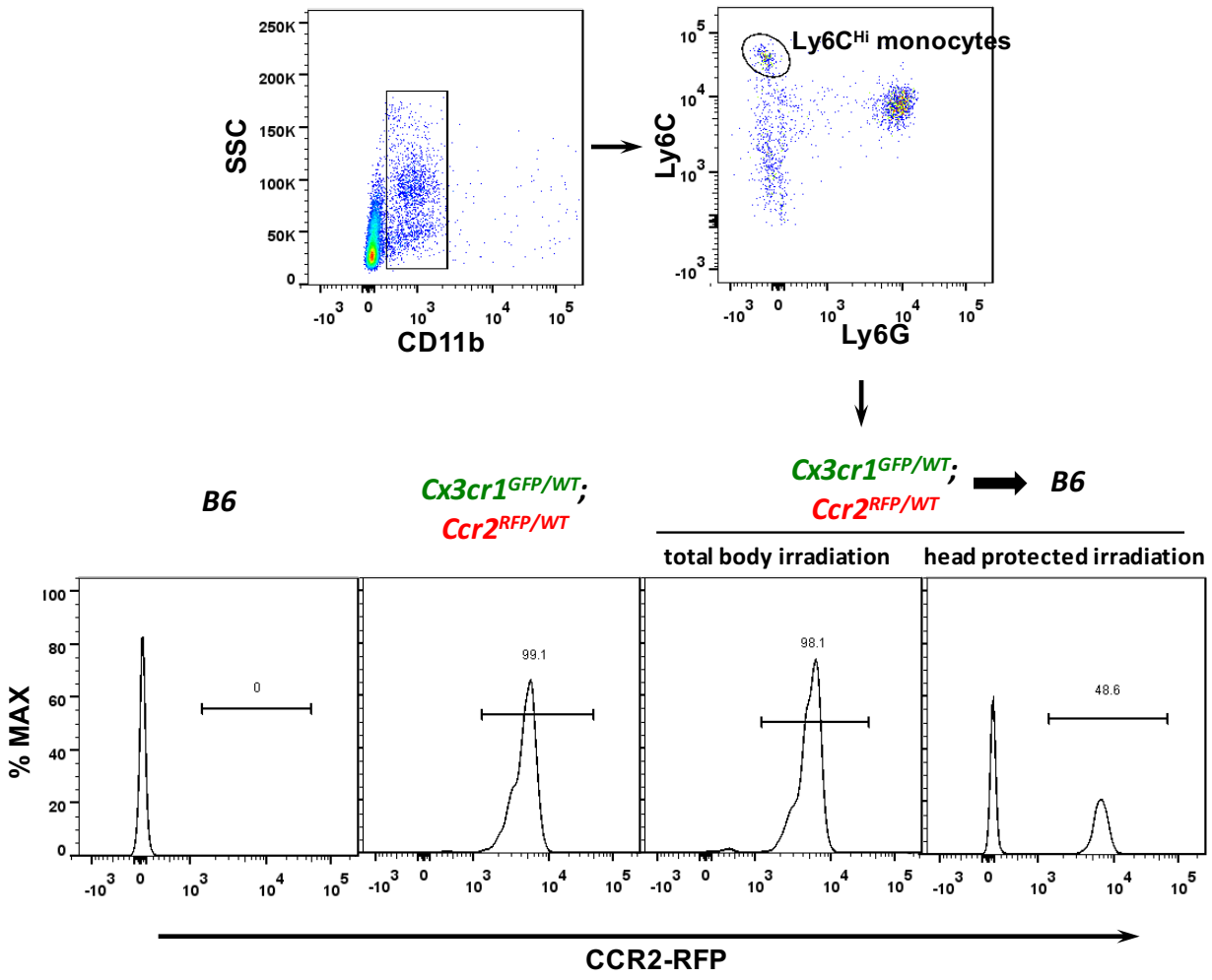

Figure S4. Bone marrow reconstitution efficiency as examined by flow cytometry. Flow cytometric analysis showing the percentage of RFP^{+} cells in total $CD11b^{+}LyG^{-}Ly6C^{Hi}$ monocytes in mice with various genotypes.

Supp. Figure S5

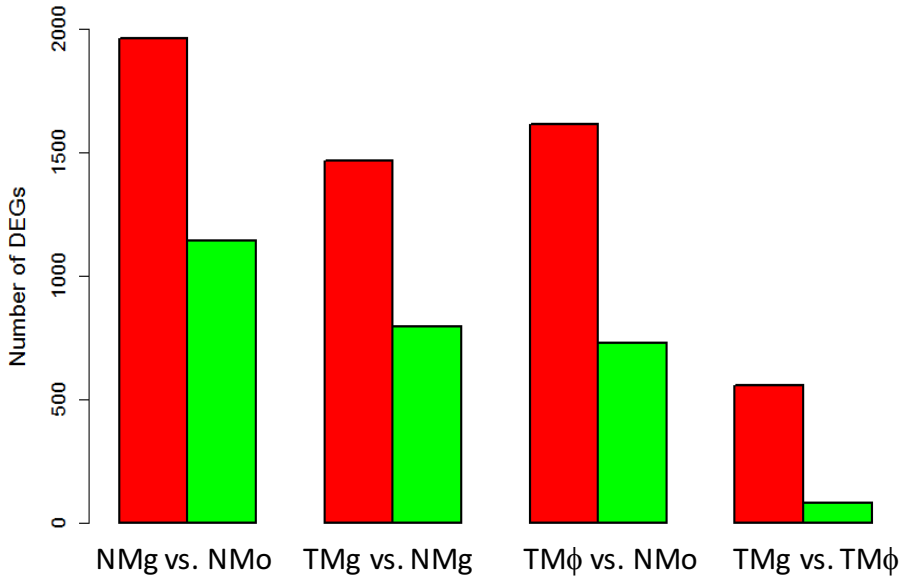

Figure S5. Significant up-regulated (red) and down-regulated (green) genes based on the pairwise comparisons.

N: naïve; T: tumor-associated; Mg: microglia; Mo: monocytes; Mϕ: macrophages.

Supp. Figure S6

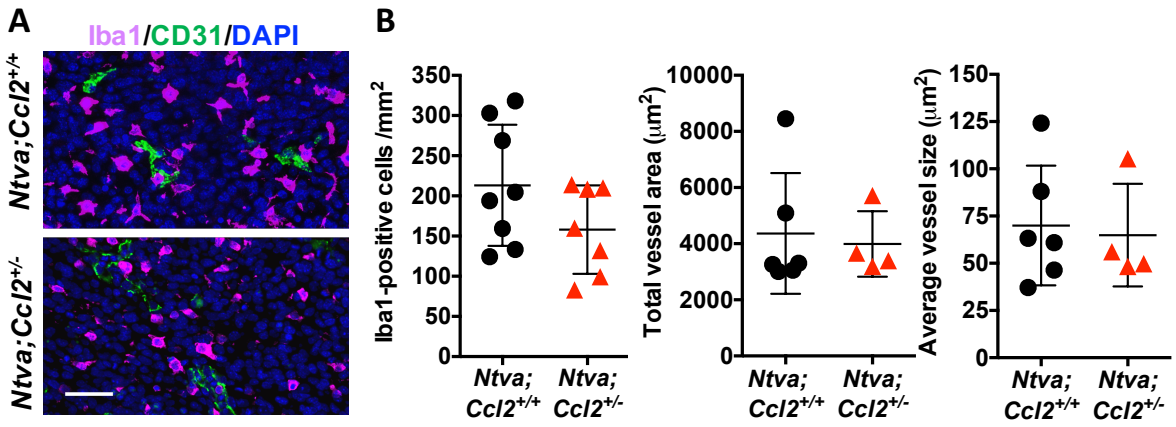

Figure S6. Loss of *Ccl2* in stroma does not prolong survival of tumor-bearing mice. (**A**) Immunohistochemistry staining of Iba1 and CD31. Scale bar = 50 μm. (**B**) Quantification of Iba1$^+$ TAMs, total vessel area and average vessel size in the tumors.

Supp. Figure S7

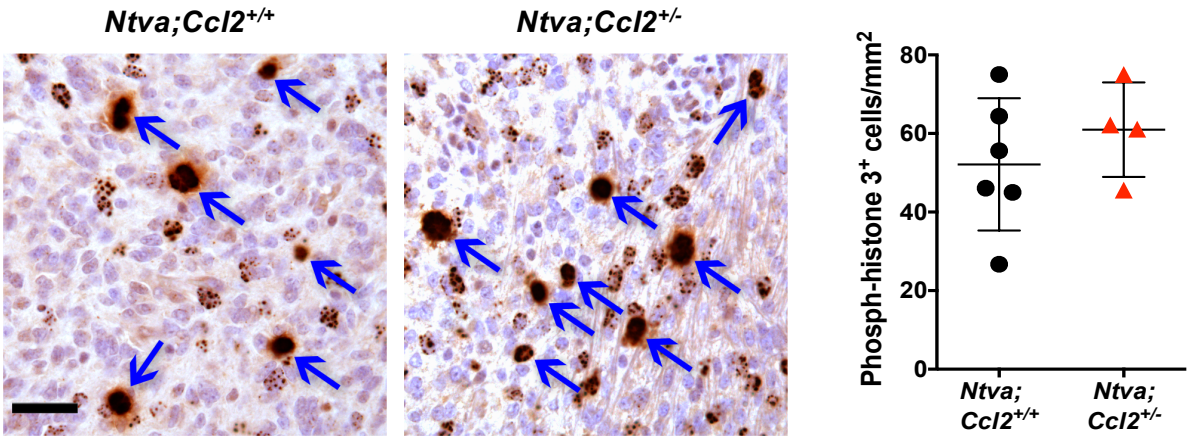

Figure S7. Immunohistochemistry staining and quantification of phosphor-histone 3 proliferating cells. Phosphor-histone 3 positive cells are pointed by the arrows. Bar = 50 µm.

Supp. Figure S8

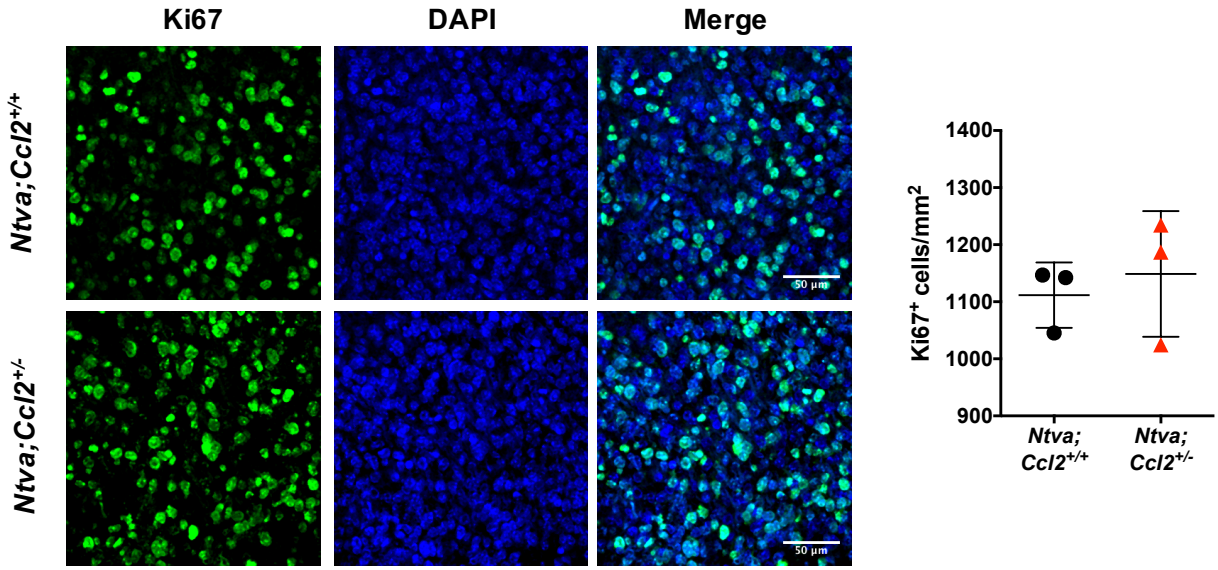

Figure S8. Immunohistochemistry staining and quantification of Ki67$^+$ proliferating cells. Bar = 50 µm.

Supp. Figure S9

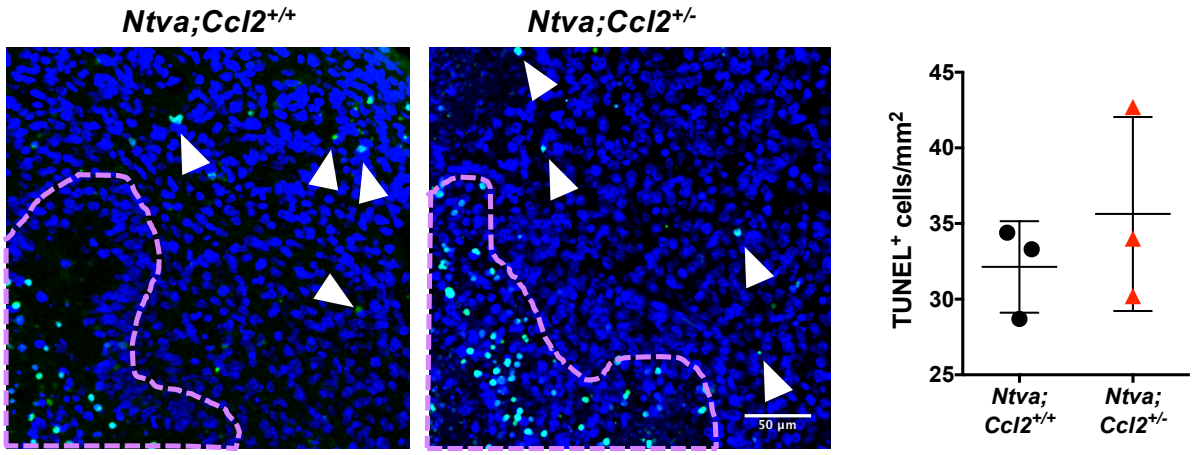

Figure S9. TUNEL staining of apoptotic cells. $TUNEL^+$ cells (green) are indicated with arrowheads. Pseudopalisading necrotic regions (circled by dotted lines) are excluded from the quantification. Bar = 50 µm.

Supp. Figure S10

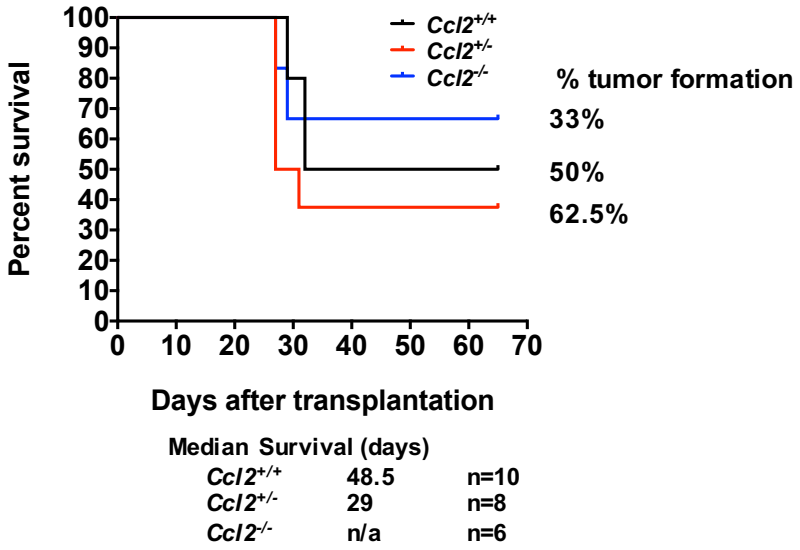

Figure S10. Survival curve of *Ccl2* WT, *Ccl2*$^{+/-}$ or *Ccl2*$^{-/-}$ mice transplanted with PDGF-driven primary murine GBM.

Supplementary Table S1. Combined *Cx3cr1* and *Ccr2* heterozygous knockout does not affect tumor development or survival.

Genotype	N	% Tumor formation	Median survival time (d)
B6 (WT)	13	54%	65
$Cx3cr1^{GFP/WT};Ccr2^{RFP/WT}$	26	63%	56

Difference not statistically significant by *t*-test.

Supp. Table S2. Significantly enriched functional pathways in tumor-associated microglia.

GeneSet	NumberOfProteinInGeneSet	ProteinFromNetwork	P-value	FDR	Nodes
Ribosome(K)	135	62	0	1.25E-14	RPL18,RPL17,RPL19,RPL14,RPL15,RPLP2,RPLP0,RPL10,RPL11,RPL12,RPS18,RPS19,RPS16,RPS17,RPS12,RPS13,RPS10,RPS11,RPS25,RPS26,RPS27,RPS28,RPS20,RPS23,RPS24,RPSA,RPS6,RPS5,RPS8,RPS7,RPL41,RPL35,RPL36,RPL37,RPL38,RPL39,RPL32,RPL31,RPL34,RPL26,RPL27,RPL24,RPL28,RPL29,RPL23,RPL22,RPL36A,RPS27L,RPL35A,UBA52,RPL9,RPL7A,RPL10A,RPL4,RPL23A,RPL37A,RPS2,RPS3,RPS3A,RPS15A,RPL27A,RPL36AL
SRP-dependent cotranslational protein targeting to membrane(R)	105	61	0	1.25E-14	RPL18,RPL17,RPL19,RPL14,RPL15,RPLP2,RPLP0,RPL10,RPL11,RPL12,RPS18,RPS19,RPS16,RPS17,RPS12,RPS13,RPS10,RPS11,RPS25,RPS26,RPS27,RPS28,RPS20,RPS23,RPS24,RPSA,RPS6,RPS5,RPS8,RPS7,RPL41,RPL35,RPL36,RPL37,RPL38,RPL39,RPL32,RPL31,RPL34,RPL26,RPL27,RPL24,RPL28,RPL29,RPL23,RPL22,RPL36A,RPL35A,UBA52,RPL9,RPL7A,RPL10A,RPL4,RPL23A,RPL37A,RPS2,RPS3,RPS3A,RPS15A,RPL27A,SEC61B
Nonsense-Mediated Decay (NMD)(R)	106	61	0	1.25E-14	RPL18,RPL17,RPL19,RPL14,RPL15,RPLP2,RPLP0,RPL10,RPL11,RPL12,RPS18,RPS19,RPS16,RPS17,RPS12,RPS13,RPS10,RPS11,RPS25,RPS26,RPS27,RPS28,RPS20,PABPC1,RPS23,RPS24,RPSA,RPS6,RPS5,RPS8,RPS7,RPL41,RPL35,RPL36,RPL37,RPL38,RPL39,RPL32,RPL31,RPL34,RPL26,RPL27,RPL24,RPL28,RPL29,RPL23,RPL22,RPL36A,RPL35A,UBA52,RPL9,RPL7A,RPL10A,RPL4,RPL23A,RPL37A,RPS2,RPS3,RPS3A,RPS15A,RPL27A
Eukaryotic Translation Initiation(R)	112	61	0	1.25E-14	RPL18,RPL17,RPL19,RPL14,RPL15,RPLP2,RPLP0,RPL10,RPL11,RPL12,RPS18,RPS19,RPS16,RPS17,RPS12,RPS13,RPS10,RPS11,RPS25,RPS26,RPS27,RPS28,RPS20,PABPC1,RPS23,RPS24,RPSA,RPS6,RPS5,RPS8,RPS7,RPL41,RPL35,RPL36,RPL37,RPL38,RPL39,RPL32,RPL31,RPL34,RPL26,RPL27,RPL24,RPL28,RPL29,RPL23,RPL22,RPL36A,RPL35A,UBA52,R

					PL9,RPL7A,RPL10A,RPL4,RPL23A,RPL37A,RPS2,RPS3,RPS3A,RPS15A,RPL27A
Eukaryotic Translation Termination(R)	84	60	0	1.25E-14	RPL18,RPL17,RPL19,RPL14,RPL15,RPLP2,RPLP0,RPL10,RPL11,RPL12,RPS18,RPS19,RPS16,RPS17,RPS12,RPS13,RPS10,RPS11,RPS25,RPS26,RPS27,RPS28,RPS20,RPS23,RPS24,RPSA,RPS6,RPS5,RPS8,RPS7,RPL41,RPL35,RPL36,RPL37,RPL38,RPL39,RPL32,RPL31,RPL34,RPL26,RPL27,RPL24,RPL28,RPL29,RPL23,RPL22,RPL36A,RPL35A,UBA52,RPL9,RPL7A,RPL10A,RPL4,RPL23A,RPL37A,RPS2,RPS3,RPS3A,RPS15A,RPL27A
Eukaryotic Translation Elongation(R)	87	60	0	1.25E-14	RPL18,RPL17,RPL19,RPL14,RPL15,RPLP2,RPLP0,RPL10,RPL11,RPL12,RPS18,RPS19,RPS16,RPS17,RPS12,RPS13,RPS10,RPS11,RPS25,RPS26,RPS27,RPS28,RPS20,RPS23,RPS24,RPSA,RPS6,RPS5,RPS8,RPS7,RPL41,RPL35,RPL36,RPL37,RPL38,RPL39,RPL32,RPL31,RPL34,RPL26,RPL27,RPL24,RPL28,RPL29,RPL23,RPL22,RPL36A,RPL35A,UBA52,RPL9,RPL7A,RPL10A,RPL4,RPL23A,RPL37A,RPS2,RPS3,RPS3A,RPS15A,RPL27A
Extracellular matrix organization(R)	248	37	0	1.57E-10	ADAMTS2,SERPINH1,MMP19,MMP16,MMP13,VCAN,COL6A2,CAPN1,COL1A2,MFAP2,COL1A1,FGB,SDC3,ADAMTS14,DCN,COL4A2,COL5A3,COL5A1,CD44,COL12A1,ITGA11,LAMB1,BMP1,LAMA4,BMP7,BGN,THBS1,MMP9,MMP8,MMP2,LOX,ITGAL,ITGB7,FN1,ITGA4,LUM,TNC
Cytokine-cytokine receptor interaction(K)	265	30	0	6.50E-06	IFNB1,IL23A,HGF,CSF2,CCL17,IL13,IL11,IL21,CCL8,CCL5,CCL7,TNFSF11,XCL1,CSF2RA,PF4,TNFSF4,TNFSF9,CD40,CD40LG,CCR2,CD70,BMP7,CXCL3,IL3RA,CXCR2,CXCR4,LTB,LTA,TNFRSF4,IL2RG
PI3K-Akt signaling pathway(K)	347	29	0.0001	0.002485341	GNG5,IFNB1,HGF,RPS6,GNB4,GNG11,COL6A2,IRS1,COL1A2,COL1A1,NR4A1,CHRM2,CHRM1,COL4A2,COL5A3,COL5A1,CREB3L1,ITGA11,LAMB1,LAMA4,THBS1,FGFR4,ITGB7,FN1,ITGA4,IL3RA,TNC,IL2RG,F2R
Focal adhesion(K)	207	19	0.0004	0.010501387	RAC2,HGF,FLNC,COL6A2,COL1A2,COL1A1,VAV3,MYL12A,COL4A2,COL5A3,COL5A1,ITGA11,LAMB1,LAMA4,THBS1,ITGB7,FN1,ITGA4,TNC

Supp Table S2.

Interferon alpha/beta signaling(R)	67	17	0	9.62E-08	ISG20,ISG15,IFNB1,USP18,BST2,IFITM2,IFITM3,IFIT3,IFIT2,IFIT1,OAS3,OAS2,STAT1,SOCS3,PSMB8,RSAD2,IRF7
ECM-receptor interaction(K)	87	17	0	3.34E-06	COL6A2,COL1A2,COL1A1,COL4A2,COL5A3,COL5A1,CD44,CD36,ITGA11,LAMB1,LAMA4,THBS1,ITGB7,FN1,ITGA4,SV2C,TNC
Integrin signalling pathway(P)	158	17	0.0001	0.00492044	RAC2,RAP2B,COL6A2,ARPC1B,COL1A2,COL1A1,COL4A2,COL5A3,COL5A1,COL12A1,RND3,ITGA11,ITGAL,ITGB7,FN1,ITGA4,ARHGAP10
Chemokine signaling pathway(K)	189	17	0.0009	0.021994349	GNG5,RAC2,GNB4,GNG11,CCL17,FGR,CCL8,CCL5,CCL7,VAV3,XCL1,PF4,CCR2,CXCL3,STAT1,CXCR2,CXCR4
Jak-STAT signaling pathway(K)	156	16	0.0003	0.010239497	IFNB1,IL23A,CSF2,IL13,IL11,IL21,SPRY4,SPRY2,CSF2RA,PIM1,STAT4,STAT1,SOCS2,SOCS3,IL3RA,IL2RG
Beta1 integrin cell surface interactions(N)	66	15	0	3.34E-06	PLAUR,COL6A2,TGFBI,COL1A2,COL1A1,FGB,COL5A1,ITGA11,LAMB1,LAMA4,THBS1,CSPG4,FN1,ITGA4,TNC
TNF signaling pathway(K)	110	13	0.0003	0.010239497	CSF2,JUNB,TRAF1,CCL5,CREB3L1,CXCL3,BCL3,MMP9,MLKL,SOCS3,RIPK3,FOS,LTA
Beta3 integrin cell surface interactions(N)	43	12	0	6.59E-06	PLAUR,SPHK1,TGFBI,COL1A2,COL1A1,FGB,LAMB1,LAMA4,CYR61,THBS1,FN1,TNC
Cell surface interactions at the vascular wall(R)	98	12	0.0004	0.010978452	SELL,LCK,PF4,CD2,APOB,CD44,FCER1G,SPN,ITGAL,FN1,ITGA4,CD244
IL12-mediated signaling events(N)	60	11	0	0.001065073	B2M,LCK,CD3E,TBX21,NOS2,GZMA,GADD45B,STAT4,STAT1,FOS,IL2RG
Urokinase-type plasminogen activator (uPA) and uPAR-mediated signaling(N)	42	9	0	0.001700745	PLAUR,HGF,MMP13,FPR1,FPR3,FPR2,FGB,MMP9,FN1
GPVI-mediated activation cascade(R)	44	8	0.0003	0.010239497	RAC2,CSF2,VAV3,CSF2RA,LCK,FCER1G,IL3RA,IL2RG
Beta2 integrin cell surface interactions(N)	29	7	0.0001	0.005082212	PLAUR,C3,TGFBI,FGB,CD40LG,CYR61,ITGAL
Validated transcriptional targets of AP1 family members Fra1 and Fra2(N)	36	7	0.0005	0.012505433	PLAUR,JUNB,COL1A2,FOSL2,DCN,MMP9,MMP2
Primary immunodeficiency(K)	36	7	0.0005	0.012505433	ZAP70,LCK,CD3E,CD40,CD40LG,CIITA,IL2RG

Supp Table S2.

Alpha9 beta1 integrin signaling events(N)	24	6	0.0003	0.01023 9497	CSF2,CSF2RA,KCNJ15,NOS2,FN1,TNC
IL12 signaling mediated by STAT4(N)	30	6	0.001	0.02434 684	IL13,CD3E,TBX21,PRF1,STAT4,FOS
Beta5 beta6 beta7 and beta8 integrin cell surface interactions(N)	17	5	0.0005	0.01273 5046	PLAUR,CYR61,ITGB7,FN1,ITGA4

Supp Table S2.

Supp. Table S3. Significantly enriched functional pathways in tumor-associated microglia and tumor-associate macrophages.

GeneSet	NumberOfProteinInGeneSet	ProteinFromNetwork	P-value	FDR	Nodes
Cytokine-cytokine receptor interaction(K)	265	27	0	4.39E-09	CCR8,VEGFA,PDGFRA,IFNA2,IFNA1,IFNA5,CCR1,CXCL2,CXCL9,KIT,CCL11,IL10,CXCL10,IL1B,PDGFC,IL1A,CCL1,CCL3,CCL2,CCL4,CXCL14,CXCL13,CXCL16,OSM,TNFRSF9,TNF,IL2RA
Mitotic Prometaphase(R)	99	25	0	5.53E-14	CDCA8,CDCA5,NCAPD2,MAD2L1,NUF2,NDC80,SPDL1,BUB1,ZWILCH,BIRC5,CCNB1,CCNB2,KNTC1,SPC24,SPC25,PLK1,KIF2C,CDK1,BUB1B,CENPN,CENPM,KIF18A,CENPF,CENPE,CENPK
Extracellular matrix organization(R)	248	24	0	8.30E-08	SERPINE1,ADAM8,SPP1,COL18A1,LAMA1,COL14A1,COL11A1,MMP15,MMP14,MMP12,COL3A1,COL7A1,COL6A1,NID1,FBLN2,ITGAX,LOXL1,CTSK,CDH1,FBN2,COL8A1,COL4A1,FBN1,COL5A2
PI3K-Akt signaling pathway(K)	347	24	0	2.09E-05	VEGFA,PDGFRA,IFNA2,IFNA1,IFNA5,PPP2R2B,SPP1,LAMA1,CCNE1,ANGPT2,COL11A1,CCND2,COL3A1,KIT,COL6A1,IGF1,PDGFC,BRCA1,CDKN1A,OSM,IL2RA,COL4A1,CREB5,COL5A2
Mitotic Metaphase and Anaphase(R)	161	21	0	6.26E-09	CDCA8,CDCA5,MAD2L1,NUF2,NDC80,SPDL1,BUB1,ZWILCH,BIRC5,KNTC1,SPC24,SPC25,PLK1,KIF2C,BUB1B,CENPN,CENPM,KIF18A,CENPF,CENPE,CENPK
Cell cycle(K)	124	19	0	4.66E-09	CCNA2,MAD2L1,CHEK1,CCNE1,CDC6,CCND2,BUB1,CCNB1,CCNB2,TTK,PKMYT1,FZR1,CDKN1A,PLK1,CDK1,MCM5,MCM6,BUB1B,CDC25C
Wnt signaling pathway(P)	272	17	0.0001	0.00166259	CDHR1,PCDH12,SFRP4,PCDHA4,PCDHB7,PCDHB5,PCDHB3,PCDHB2,PCDHB15,PCDHB10,CDH17,WNT2,SMARCA1,HELLS,TNF,CDH1,FRZB
PLK1 signaling events(N)	44	15	0	1.92E-11	AURKA,NDC80,CLSPN,TPX2,BUB1,CCNB1,PRC1,FZR1,SPC24,PLK1,CDK1,ECT2,BUB1B,CENPE,CDC25C
Mitotic G1-G1/S phases(R)	126	15	0	6.62E-06	PRIM1,POLE,MYBL2,CCNE1,TOP2A,CDC6,RRM2,CCNB1,PKMYT1,CDKN1A,MCM8,CDK1,MCM5,MCM6,CKS1B

HTLV-I infection(K)	260	15	0.0005	0.008183346	POLE,MAD2L1,PDGFRA,CHEK1,MYBL2,CCND2,CREM,CCNB2,WNT2,CDKN1A,EGR1,EGR2,BUB1B,TNF,IL2RA
Cell Cycle Checkpoints(R)	116	14	0	1.34E-05	MAD2L1,CHEK1,CLSPN,CDC6,CCNB1,CCNB2,PKMYT1,CDKN1A,MCM8,CDK1,MCM5,MCM6,BUB1B,CDC25C
Chemokine signaling pathway(K)	189	14	0.0001	0.001242821	CCR8,CCR1,CXCL2,CXCL9,CCL11,CXCL10,CCL1,CCL3,CCL2,CCL4,CXCL14,CXCL13,CXCL16,SHC2
Focal adhesion(K)	207	14	0.0002	0.002896513	VEGFA,PDGFRA,SPP1,LAMA1,COL11A1,CCND2,COL3A1,COL6A1,IGF1,PDGFC,RASGRF1,SHC2,COL4A1,COL5A2
Beta1 integrin cell surface interactions(N)	66	13	0	1.94E-07	VEGFA,SPP1,COL18A1,LAMA1,COL11A1,COL3A1,COL7A1,COL6A1,NID1,TGM2,COL4A1,FBN1,COL5A2
Viral carcinogenesis(K)	206	13	0.0005	0.008183346	HIST1H2BM,HIST1H2BK,HIST1H2BL,CCNA2,CCR8,CHEK1,CCNE1,CCND2,HIST1H2BH,CDKN1A,CDK1,EGR2,CREB5
Cadherin signaling pathway(P)	100	12	0	7.95E-05	CDHR1,PCDH12,PCDHA4,PCDHB7,PCDHB5,PCDHB3,PCDHB2,PCDHB15,PCDHB10,CDH17,WNT2,CDH1
Oocyte meiosis(K)	113	12	0	2.21E-04	AURKA,MAD2L1,CCNE1,BUB1,IGF1,CCNB1,CCNB2,PKMYT1,PLK1,CDK1,CAMK2B,CDC25C
S Phase(R)	119	12	0	3.44E-04	PRIM1,CDCA5,LIG1,POLE,CDC6,FZR1,CDKN1A,MCM8,MCM5,MCM6,CKS1B,APEX1
p53 signaling pathway(K)	68	11	0	1.46E-05	SERPINE1,CHEK1,GTSE1,CCNE1,CCND2,RRM2,IGF1,CCNB1,CCNB2,CDKN1A,CDK1
Progesterone-mediated oocyte maturation(K)	89	11	0	1.49E-04	CCNA2,MAD2L1,BUB1,IGF1,CCNB1,CCNB2,PKMYT1,FZR1,PLK1,CDK1,CDC25C
Toll-like receptor signaling pathway(K)	106	11	0	5.10E-04	IFNA2,IFNA1,IFNA5,SPP1,CXCL9,CXCL10,IL1B,CCL3,CCL4,CTSK,TNF
Mitotic G2-G2/M phases(R)	111	11	0	7.08E-04	AURKA,CCNA2,MYBL2,CCNB1,CCNB2,PKMYT1,PLK1,CDK1,FOXM1,CENPF,CDC25C
FOXM1 transcription factor network(N)	41	10	0	1.68E-06	CCNA2,CCNE1,BIRC5,CCNB1,CCNB2,PLK1,CDK1,CKS1B,FOXM1,CENPF
Synthesis of DNA(R)	95	10	0	8.96E-04	PRIM1,LIG1,POLE,CDC6,FZR1,CDKN1A,MCM8,MCM5,MCM6,APEX1
Factors involved in megakaryocyte development and platelet production(R)	112	10	0.0002	0.002896513	KIFC1,KIF5A,IFNA2,IFNA1,IFNA5,KIF2C,KIF11,KIF15,KIF18A,CENPE

Supp. Table S3.

Neurotransmitter Receptor Binding And Downstream Transmission In The Postsynaptic Cell(R)	132	10	0.0006	0.009068257	GRIP1,CACNG4,GRIA4,GABRB3,GRIK2,GRIK5,RASGRF1,GRIN1,GABRG3,CAMK2B
FoxO signaling pathway(K)	133	10	0.0006	0.009068257	FOXG1,BNIP3,CCND2,IGF1,CCNB1,CCNB2,IL10,CDKN1A,PLK2,PLK1
Hepatitis B(K)	146	10	0.0013	0.015589762	CCNA2,IFNA2,IFNA1,IFNA5,CCNE1,BIRC5,CDKN1A,EGR2,TNF,CREB5
E2F transcription factor network(N)	68	9	0	4.90E-04	SERPINE1,CCNA2,MYBL2,CCNE1,CDC6,RRM2,BRCA1,CDKN1A,CDK1
p73 transcription factor network(N)	74	9	0	7.60E-04	SERPINE1,CCNA2,CHEK1,BUB1,CCNB1,CDKN1A,PLK1,CDK1,GDF15
Protein digestion and absorption(K)	89	8	0.0007	0.009448757	COL18A1,COL14A1,COL11A1,COL3A1,COL7A1,COL6A1,COL4A1,COL5A2
Aurora A signaling(N)	31	7	0	1.87E-04	AURKA,TPX2,DLGAP5,BIRC5,TACC3,FZR1,BRCA1
ATR signaling pathway(N)	37	7	0	4.73E-04	CCNA2,CHEK1,PPP2R2B,CLSPN,CDC6,PLK1,CDC25C
Aurora B signaling(N)	40	7	0	6.59E-04	AURKA,CDCA8,NCAPD2,NDC80,BUB1,BIRC5,KIF2C
Downstream signaling in naive CD8+ T cells(N)	63	7	0.0005	0.007776291	IFNA2,IFNA1,IFNA5,EGR1,TNFRSF9,TNF,IL2RA
Amphetamine addiction(K)	68	7	0.0007	0.009448757	ARC,FOSB,GRIA4,GRIN1,CACNA1C,CAMK2B,CREB5
APC/C-mediated degradation of cell cycle proteins(R)	80	7	0.0018	0.019819798	AURKA,MAD2L1,CCNB1,FZR1,PLK1,CDK1,BUB1B
Validated transcriptional targets of deltaNp63 isoforms(N)	46	6	0.0005	0.008173345	TOP2A,AXL,CCNB2,IL1A,VDR,HELLS
HIF-2-alpha transcription factor network(N)	33	5	0.0008	0.010081148	SERPINE1,VEGFA,MMP14,BHLHE40,APEX1
DNA replication(K)	36	5	0.0011	0.013659778	PRIM1,LIG1,POLE,MCM5,MCM6
IL23-mediated signaling events(N)	36	5	0.0011	0.013659778	CXCL9,IL1B,CCL2,TNF,CD4

Supp. Table S3.

Double-Strand Break Repair(R)	22	4	0.0014	0.016312148	LIG1,BRIP1,BRCA1,APEX1
Signaling events mediated by PRL(N)	23	4	0.0016	0.017570473	CCNA2,CCNE1,CDKN1A,EGR1
Alpha9 beta1 integrin signaling events(N)	24	4	0.0019	0.020490958	ADAM8,VEGFA,SPP1,TGM2
il-10 anti-inflammatory signaling pathway(B)	12	3	0.0023	0.025074067	IL10,IL1A,TNF

Supp. Table S3.

Supp. Table S4. Significantly enriched functional pathways in tumor-associated macrophages.

GeneSet	NumberOfProteinInGeneSet	ProteinFromNetwork	P-value	FDR	Nodes
Extracellular matrix organization(R)	248	34	0	1.40E-08	LTBP4,F11R,LAMC3,LAMC1,ELN,LAMB2,BMP4,LAMA2,FGF2,COL15A1,HSPG2,COL19A1,MMP3,TGFB2,NCAM1,MFAP5,ITGAE,ITGB5,TIMP2,ITGB8,EFEMP2,NTN4,ITGA3,ITGA9,BCAN,SDC4,DDR2,SDC2,CTSL,SDC1,CTSD,JAM3,COL13A1,SPARC
Pathways in cancer(K)	398	31	0	0.00340956	GNG7,CTNNA2,VEGFB,LAMC3,JUN,LAMC1,GNAI1,LAMB2,BMP4,LAMA2,GLI2,EDNRA,TGFA,FGF2,RAD51,CCND1,IL6,FZD2,FZD7,FZD6,GNA12,ARNT2,CXCL12,TGFB2,CDKN2A,EGFR,WNT5A,AXIN2,BRCA2,ITGA3,RALGDS
PI3K-Akt signaling pathway(K)	347	26	0.0003	0.010041162	OSMR,GNG7,VEGFB,LAMC3,LAMC1,IFNA1,LAMB2,IFNA6,IFNA4,GYS1,PPP2R2C,EPHA2,LAMA2,FGF2,GHR,CCND1,IL6,EGFR,NGF,ITGB5,ITGB8,TEK,ITGA3,ITGA9,SGK1,FLT4
Wnt signaling pathway(P)	272	25	0	0.001872781	EDN1,GNG7,CTNNA2,PCDH10,PCDHB6,PCDHB4,MYCN,CCND1,NKD1,PCDHB11,DCHS1,FAT3,PCDHB16,FZD2,FZD7,FZD6,CDH13,CDH19,WNT5A,AXIN2,PCDH1,PCDH9,CDH4,CDH5,BMPR1A
Proteoglycans in cancer(K)	204	22	0	7.42E-04	ERBB4,CD63,PLAU,FGF2,CCND1,IL12B,HSPG2,FZD2,FZD7,FZD6,HBEGF,TGFB2,EGFR,PLCE1,WNT5A,ITGB5,SRC,SDC4,SDC2,GPC3,CTSL,SDC1
Cytokine-cytokine receptor interaction(K)	265	20	0.0012	0.025201288	OSMR,VEGFB,IFNA1,IFNA6,IFNA4,TNFRSF11A,GHR,ACKR3,IL12B,IL6,CXCL12,TGFB2,EGFR,TNFRSF17,CNTFR,IL12RB1,IL21R,TNFSF13B,FLT4,BMPR1A
Focal adhesion(K)	207	19	0.0002	0.007865571	VEGFB,LAMC3,JUN,LAMC1,LAMB2,LAMA2,CCND1,PARVA,EGFR,MYL2,ITGB5,SRC,ITGB8,ITGA3,ITGA9,TLN2,PAK3,SHC3,FLT4
Cell adhesion molecules (CAMs)(K)	144	18	0	7.42E-04	F11R,CD34,NEO1,NLGN1,CTLA4,NCAM1,ITGB8,ITGA9,SDC4,SDC2,NRXN2,SDC1,CLDN1,CNTN1,JAM3,CDH4,CDH5,NFASC

Metabolism of carbohydrates(R)	223	18	0.001	0.022172798	PRELP,HS3ST3B1,ALDOC,GYS1,EPM2A,CHST11,HSPG2,B4GALT2,BCAN,SDC4,SDC2,GPC2,GPC3,GPC6,CHST2,CHST1,SDC1,HS6ST2
Cadherin signaling pathway(P)	100	17	0	4.51E-05	CTNNA2,PCDH10,PCDHB6,PCDHB4,PCDHB11,DCHS1,FAT3,PCDHB16,FZD2,FZD7,FZD6,CDH13,CDH19,WNT5A,PCDH1,PCDH9,CDH5
Hippo signaling pathway(K)	153	17	0	0.00340956	CTNNA2,PPP2R2C,BMP4,GLI2,CCND1,PARD3,NKD1,FZD2,WWTR1,FZD7,FZD6,TGFB2,WNT5A,SOX2,AXIN2,TEAD1,BMPR1A
Assembly of the primary cilium(R)	171	15	0.0012	0.025201288	CC2D2A,WDR60,TUBB4A,NPHP1,TTC26,DYNLL2,WDR35,WDR34,BBS12,IFT74,TUBG1,BBS5,BBS7,TTC8,ARL6
Axon guidance(K)	127	14	0.0002	0.008081533	GNAI1,EPHA2,SEMA6A,SEMA6C,SEMA3F,SLIT2,SEMA4C,PLXNA1,CXCL12,UNC5B,PLXNB3,NTN4,PAK3,DPYSL5
Tight junction(K)	138	14	0.0004	0.01411513	AMOTL1,F11R,MAGI1,CTNNA2,GNAI1,PPP2R2C,PARD3,TJP1,MYL2,SRC,MYH10,CLDN1,JAM3,YES1
Rheumatoid arthritis(K)	90	12	0.0001	0.006377464	JUN,ATP6V0E2,TNFRSF11A,IL6,CTLA4,ATP6V0A4,MMP3,CXCL12,TGFB2,TEK,CTSL,TNFSF13B
Alzheimer disease-presenilin pathway(P)	111	12	0.0006	0.01888204	CTNNA2,BACE2,ERBB4,NOTCH4,PCSK6,FZD2,FZD7,FZD6,APBB2,LRP3,LRP1B,WNT5A
L1CAM interactions(R)	79	11	0.0001	0.007113544	LAMC1,SCN1B,NRP2,RPS6KA6,EGFR,NCAM1,SRC,ITGA9,CNTN1,DCX,NFASC
Hypertrophic cardiomyopathy (HCM)(K)	83	11	0.0002	0.008081533	LAMA2,CACNG8,CACNG7,IL6,TGFB2,MYL2,ITGB5,ITGB8,ITGA3,ITGA9,DES
ECM-receptor interaction(K)	87	11	0.0003	0.010542376	LAMC3,LAMC1,LAMB2,LAMA2,HSPG2,ITGB5,ITGB8,ITGA3,ITGA9,SDC4,SDC1
Cell surface interactions at the vascular wall(R)	98	11	0.0008	0.020187993	F11R,GAS6,SLC3A2,SLC7A8,SRC,TEK,ITGA3,MERTK,SLC7A11,JAM3,YES1
Complement and coagulation cascades(K)	69	10	0.0002	0.008081533	C1QC,C5AR1,C1QA,C1QB,F3,TFPI,PLAU,C3AR1,KNG1,C1S
Mineral absorption(K)	51	9	0.0001	0.006377464	MT1A,MT1E,MT1H,MT1G,MT1F,MT1M,MT1X,MT2A,SLC40A1
Notch signaling pathway(N)	52	9	0.0001	0.006466981	NOTCH4,CCND1,ADAM12,JAG2,DLK1,JAG1,MFAP5,CNTN1,DNER

Supp. Table S4

Semaphorin interactions(R)	65	9	0.0005	0.016841756	SEMA6A,PLXNA1,PLXNB3,MYH10,PAK3,RHOC,TREM2,DPYSL5,DPYSL4
Epithelial cell signaling in Helicobacter pylori infection(K)	68	9	0.0007	0.020187993	F11R,JUN,ATP6V0E2,TJP1,HBEGF,ATP6V0A4,EGFR,SRC,JAM3
Cell junction organization(R)	69	9	0.0008	0.02062129	F11R,FERMT2,FBLIM1,PARVA,PARD3,LIMS2,CDH13,CDH4,CDH5
AP-1 transcription factor network(N)	70	9	0.0009	0.021868605	EDN1,JUN,PLAU,CCND1,IL6,MT2A,CDKN2A,ATF3,NTS
Prion diseases(K)	36	8	0	0.003938377	C1QC,C1QA,C1QB,LAMC1,HSPA1A,IL6,NCAM1,PRNP
Urokinase-type plasminogen activator (uPA) and uPAR-mediated signaling(N)	42	7	0.0008	0.020187993	PLAU,VLDLR,MMP3,EGFR,ITGB5,SRC,ITGA3
Syndecan-4-mediated signaling events(N)	32	6	0.001	0.022172798	TFPI,FGF2,ADAM12,FZD7,CXCL12,SDC4
Proteoglycan syndecan-mediated signaling events(N)	4	3	0.0004	0.01411513	SDC4,SDC2,SDC1

Supplemental Information: RNA Sequencing analysis

RNA-seq library preparation and sequencing

Original source RNA samples were assayed using the Agilent Eukaryotic Total RNA 6000 Pico assay (Agilent Technologies, Santa Clara, CA) and were of reasonable quality with an RNA Integrity Number (RIN) values higher than 9.5. Source RNA aliquots of 2 ~ 436 ng total RNA were DNase-treated using the TURBO DNA-free kit (Ambion, Austin, TX) eliminating residual DNA prior to cDNA synthesis. Post DNase, both RNA quality and yield were re-evaluated with the Agilent Eukaryotic Total RNA 6000 Pico and the Quant-iT™ RNA assay kit on a Qubit™ Fluorometer (Life Technologies Corporation, Carlsbad, CA). Starting with 25ng DNase-treated total RNA when available or less, we employed the Ovation® RNA-Seq v2 method for cDNA synthesis (NuGen, San Carlos, CA). First-strand cDNA synthesis included 5 µl RNA, 2 µl 1st strand primer and incubated at 65ºC for 5 minutes to denature, and cooled to 4ºC and incubated on ice for primer annealing. Next, 2.5 µl first strand buffer mix and 0.5 µl first strand enzyme mix were added and incubated as follows: 4ºC for 1 minute, 25ºC for 10 minutes, 42ºC for 10 minutes, and reaction stop at 70ºC for 15 minutes. Post first-strand synthesis, the reaction was placed on ice. Second-strand cDNA synthesis included 9.7 µl second strand buffer mix and 0.3 µl second strand enzyme mix to the first strand reaction. This reaction was incubated as follows: 4ºC for 1 minute, 25ºC for 10 minutes, 50ºC for 30 minutes, reaction stop at 80ºC for 20 minutes, and the reaction was stored on ice. cDNA was recovered by the addition of 1.8X volumes (32 µl) of Agencourt RNAClean XP beads (Beckman Coulter Inc., Pasadena, CA) and a 10 minute incubation at 25ºC on lab rotator. cDNA-bound paramagnetic beads were placed on a DynaMag™ magnet (Dynal®, Invitrogen, Carlsbad, CA) allowing beads to form a small pellet. Supernatant was discarded and beads were washed three times with 200 µl of freshly prepared 70% ethanol and allowed to dry. With the cDNA bound to bead, single primer isothermal amplification (SPIA) was achieved by adding 20 µl SPIA buffer mix, 10 µl SPIA primer mix, and 10 µl SPIA enzyme mix. The amplification reaction conditions were as follows: 4ºC for 1 minute, 47ºC for 60 minutes, reaction stop at 80ºC for 20 minutes and held at 4ºC. The beads were pelleted by incubation on a DynaMag™ magnet, and

40 µl of the cleared supernatant was recovered. cDNA was purified by adding 200 µl PB buffer (Qiagen, Venlo, Limburg) and passed through a MinElute column (Qiagen, Venlo, Limburg). The column was washed twice with 750 µl PE buffer, and cDNA was eluted from the column in 30 µl Elution Buffer (Qiagen, Venlo, Limburg). Illumina library construction techniques are explained in Cabanski et al., (1) using our modified dual-same indexing scheme. Finally, samples were sequenced on the HiSeq 2000 at 2 × 101 bp in the paired ends. Illumina HiSeq Control Software 2.0.12.0 and Real-Time Analysis 1.17.21.3 where used for sequencing and raw instrument data processing.

RNA-seq read alignment and transcript assembly

Quality of raw sequencing data in the paired-end mode was assessed using FastQC version 0.10.0 (http://www.bioinformatics.babraham.ac.uk/projects/fastqc/). 100-bp RNA-seq sequencing reads from all libraries were trimmed using the Flexible Barcode and Adapter Remover software (FLEXBAR version 2.29) (2), and the SPIA adaptor sequence was removed in the 5' end of reads before read alignment. These trimmed reads were subsequently mapped by TopHat version 2.0.8 (3), incorporating Bowtie 2 version 2.1.0 (4), against the mouse reference genome build mm9 that was downloaded from the UCSC genome browser. The default parameters were used, and the mouse annotation database from Ensembl release 67 was used for reference-based transcriptome assembly and subsequent gene expression analysis, described in the next section. *De novo* transcript sequence reconstruction was performed from sequenced cDNA fragments of RNA-seq for unannotated transcript discovery, using the cufflinks assembler (version 2.1.1) with the following parameters, "--num-threads 4 --max-bundle-length 10000000" (5). The compressed binary alignment files in BAM were summarized by SAMStat version 1.08 and SAM tools version 0.1.16 (6). Downstream BAM files were converted and handled using Picard utilities of version 1.85 8. (http://broadinstitute.github.io/picard/).

Gene and isoform expression analysis by RNA-seq

Gene and isoform expression levels were calculated using Cufflinks version 2.1.1 (7), which assembles the mapped fragments from RNA-seq into transcripts and estimates the relative abundances of those transcripts in cells. Transcripts from mitochondrial and ribosomal RNA genes were masked and not included. Cross-replicate variability in their fragment counts was estimated with 3 replicate samples, and their final abundances in cells were computed in FPKM (Fragments Per Kilobase of exon model per Million mapped fragments). The GTF (General Transfer Format) from Ensembl release 67 was used for genome-wide transcriptome quantification of protein-coding genes, annotated in mm9, including alternative transcript isoform expression estimation.

Differential expression analysis by RNA-seq

In order to compare gene and transcript expression under two conditions, the annotated GTF above was fed to the cuffdiff algorithm in Cufflinks to measure the fold change of the coding genes. Final differentially expressed genes (DEGs) were listed with their expected fragment numbers (or FPKMs). To identify overlapping or unique DEGs, a minimum Log 2 fold change of 2 and P-value ≤ 0.01 were used as cut-off value in the pairwise comparisons. A cross comparison was then applied to identify overlapping and unique DEGs between tumor-associated microglia and macrophages. The biological processes enriched among the overlapping DEGs were searched against a variety of databases using the Reactome FIViz plugin (8) in Cytoscape (9). The significance of GO (gene ontology) terms was determined based on P-value (≤ 0.001) and FDR (≤ 0.025). The number of unique DEGs specific to tumor-associated microglia, tumor-associated macrophages, and common to both in a defined functional category are presented. The FPKM data, along with experimental information is deposited in the NCBI Sequence Read Archive (SRA) database under accession number #.

Reference:

1. Cabanski CR, Magrini V, Griffith M, Griffith OL, McGrath S, Zhang J, et al. cDNA hybrid capture improves transcriptome analysis on low-input and archived samples. J Mol Diagn 2014;16(4):440-51.
2. Dodt M, Roehr JT, Ahmed R, Dieterich C. FLEXBAR-Flexible Barcode and Adapter Processing for Next-Generation Sequencing Platforms. Biology (Basel) 2012;1(3):895-905.
3. Kim D, Pertea G, Trapnell C, Pimentel H, Kelley R, Salzberg SL. TopHat2: accurate alignment of transcriptomes in the presence of insertions, deletions and gene fusions. Genome Biol 2013;14(4):R36.
4. Langmead B, Salzberg SL. Fast gapped-read alignment with Bowtie 2. Nat Methods 2012;9(4):357-9.
5. Trapnell C, Williams BA, Pertea G, Mortazavi A, Kwan G, van Baren MJ, et al. Transcript assembly and quantification by RNA-Seq reveals unannotated transcripts and isoform switching during cell differentiation. Nat Biotechnol 2010;28(5):511-5.
6. Li H, Handsaker B, Wysoker A, Fennell T, Ruan J, Homer N, et al. The Sequence Alignment/Map format and SAMtools. Bioinformatics 2009;25(16):2078-9.
7. Trapnell C, Hendrickson DG, Sauvageau M, Goff L, Rinn JL, Pachter L. Differential analysis of gene regulation at transcript resolution with RNA-seq. Nat Biotechnol 2013;31(1):46-53.
8. Wu G, Feng X, Stein L. A human functional protein interaction network and its application to cancer data analysis. Genome Biol 2010;11(5):R53.
9. Smoot ME, Ono K, Ruscheinski J, Wang PL, Ideker T. Cytoscape 2.8: new features for data integration and network visualization. Bioinformatics 2011;27(3):431-2.